SYNCHRONIZATION OF ps ELECTRON BUNCHES AND fs LASER PULSES USING A PLASMONICS-ENHANCED LARGE-AREA PHOTOCONDUCTIVE DETECTOR

E. J. Curry*, M. Jarrahi, P. Musumeci, N. T. Yardimci†, UCLA, Los Angeles, CA 90095, USA
B. T. Jacobson, RadiaBeam Technologies, Santa Monica, CA 90405, USA

Abstract

Temporal synchronization between short relativistic electron bunches and laser pulses at the ps and sub-ps level is required for accelerator applications like inverse Compton scattering based light sources. Photoconductive antennas with THz and sub-THz bandwidth which are gated by fs lasers provide this level of timing resolution. This paper describes the operating principals of the diagnostic along with bench-top experimental results with recently developed plasmonics-enhanced large-area devices. A vacuum chamber with robust electronic noise reduction has been designed for upcoming beam-based experiments.

INTRODUCTION

Modern high-brightness photo-injectors have evolved to produce bunched beams of relativistic electrons with ps and sub-ps duration, while commercial laser technology has reduced pulse lengths of high-power IR sources to 100 fs and below. These two advances have led to a merging of these disciplines into a new scientific field where each core technology must operate at peak performance and be synchronized in time with a resolution better than the pulse lengths involved, such as in inverse Compton scattering, where the electron bunch and laser pulse must arrive simultaneously and collide at the interaction point.

SYNCHRONIZATION MEASUREMENT METHODS

A traditional way for synchronizing electron beam and laser pulses is by using signals from button or stripline beam position monitor for electrons timing [1] while monitoring laser pulses with a biased photodiode. To acquire sub-ps resolution, optical and cable delays must be characterized and the analog signals must be sampled by a high-bandwidth oscilloscope.

Instead of directly measuring beam or laser signal, several techniques have been developed for bunch length measurements and synchronization known as electro-optic sampling (EOS) methods, where the bunch profile is encoded in a signal [2]. Each scheme exploits the changes in optical properties, e.g. birefringence, of some material due to the presence of the passing electric field of the beam. Our EOS setup uses a Wollaston prism configured for doubly-balanced diode detection.

Another method for beam and laser synchronization uses a photoconductive antenna (PCA) which behaves like an optically gated THz sensor. The gate is provided by a fs laser pulse which allows charge flow in a photoconductive substrate for the duration of the illuminating pulse. THz fields generated by the ps or sub-ps electron bunches can be extracted via a transition radiation foil, or measured directly by placing the PCA detector in close proximity to the electron beam. Bunch length measurements have been made [3] using transition radiation and specially designed radially polarized PCA detectors [4]. However, we pursue directly measuring the Coulomb field of the electron bunches by placing the detector inside of the beam vacuum chamber [5].

EXPERIENCE WITH COMMERCIALLY AVAILABLE PCA SENSORS

Last year we made attempts to adapt a commercially available PCA sensor for beam measurements at the UCLA Pegasus beamline [6]. The sensor had a 5 μm gap in the dipole antenna structure. A large laser spot illuminating a movable pin-hole was used to limit the probe beam size and position the spot in the dipole gap. Bench test of the device mounted in this manner [5] showed this detector should be sensitive to the peak THz field amplitudes excited in close proximity to the Pegasus beam.

However, these beam measurements were unsuccessful. Three issues have been identified that contributed to the failed measurement attempt: maintaining laser alignment one the pinhole assembly was pumped down, the presence of large electronic noise backgrounds, and the overall device sensitivity to THz fields. Over the past year, we have addressed each of these issues, as described in the remainder of this contribution.

DESCRIPTION OF PLASMONICS-ENHACED LARGE-AREA PHOTOCONDUCTIVE DETECTORS

Incorporation of plasmonic contact electrodes into PCAs has been proven to be an efficient concept to increase the sensitivity and responsivity of the conventional photoconductive detectors [7]. In this project, a novel large-area plasmonic photoconductive device based on a 2-D plasmonic nano-antenna array is used. By using a large-area design, the optical beam doesn't have to be focused tightly anymore. Therefore, the device can accommodate higher optical pump power levels without any thermal breakdown and offers much easier optical alignment. Moreover, the nano-antennas are designed to have low RC parasitic loading; hence, the detector offers a

*ejcurry99@gmail.com
†yardimci@ucla.edu (photoconductive detector design)

ISBN 978-3-95450-177-9

broad detection bandwidth [8]. The plasmonic nano-antennas are designed to increase the interaction between the optical beam and the THz pulse. Therefore, high responsivities can be achieved with this detector.

The schematic design of the plasmonic-enhanced detector is shown in Fig. 1. It is 0.5 mm x 0.5 mm in area and fabricated on top of a low-temperature-grown GaAs substrate. The geometry of the plasmonic nano-antennas is designed to excite the surface-plasmon waves at 800 nm wavelength. Therefore, extraordinary optical absorption is achieved at this wavelength, providing a much shorter average path length for the photo-generated carriers. The gap between nano-antenna tips is chosen to optimize the optical transmission and the induced electric fields at THz frequencies. Thus, when a THz pulse is incident on the detector a strong electric field is induced between nano-antenna tips. Since the average path length of photo-generated carriers is short and the THz fields induced within the device active area is strong, the majority of the photo-generated carriers can be drifted to the contact electrodes in less than a picosecond. Hence, very high responsivities can be achieved.

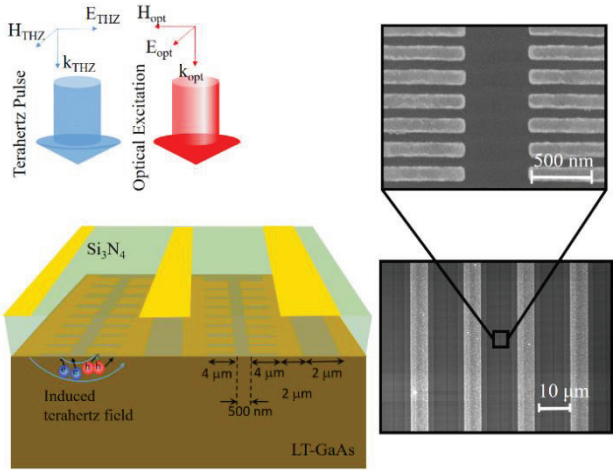

Figure 1: Schematic diagram of the presented large-area plasmonic photoconductive detector (left). SEM images of the 2D plasmonic nano-antenna array (right).

Moreover, the length of the dipole antennas is chosen to be much smaller (4 µm) than the THz wavelength to provide broadband radiation detection. Experimentally, we could observe signal up to 6 THz using a broad-band source.

The 2D nano-antenna arrays are connected to interdigitated lines. A Si_3N_4 anti-reflection (AR) coating is used to further enhance the optical transmission. Strips of metal are applied on top of the AR coating to block the laser light directly above every second gap between the interdigitated lines. This eliminates charge flowing in the opposite direction which interferes destructively with the current generated by the plasmonic nano-antennas. SEM images of the plasmonic nano-antenna array are shown in Fig. 1 (right).

CHARACTERIZATION OF THREE PLASMONICS-ENHANCED PHOTO-CONDUCTIVE DEVICES

We present measurements of THz detection using three PCA structure types. The primary PCA used in this experiment is described above and has been optimized for THz detection. Another PCA chip design, optimized for THz emission rather than detection, was available in two sizes of active area. A photo of all three mounted is shown in Fig. 2. We include these additional measurements for comparison with the PCA optimized for THz detection performance and to provide insight into the potential scaling of the PCA performance with area of the active region.

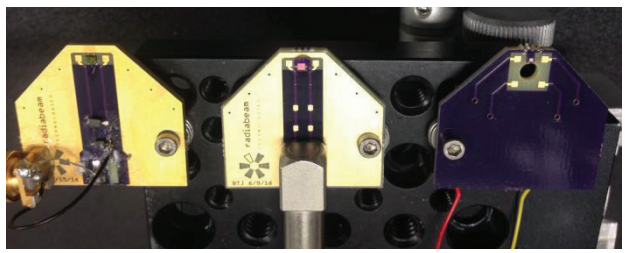

Figure 2: Photograph of the three PCA designs used for the measurements presented here. At left is the PCA optimized for THz detection, in the middle is the large area PCA optimized for THz emission, and at right is the small area PCA optimized for THz emission.

The THz pulse was produced via pulse-front-tilted optical rectification of 800 nm IR pulses in stoichiometric lithium niobate (sLN) and focused using a pair of off-axis parabolic mirrors (OAP), as shown in Fig. 3. To characterize the THz source, we performed EOS measurements of the near-single cycle pulse using a balanced detection scheme with a 0.5 mm thick ZnTe crystal.

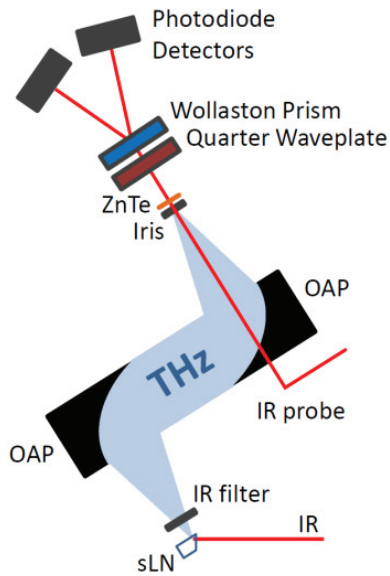

Figure 3: Diagram of THz generation and balanced detection set-up for EOS. The ZnTe crystal is replaced by a PCA for antenna measurements.

ISBN 978-3-95450-177-9

For each measurement, an iris was used for coarse alignment of the board relative to the THz focus, followed by fine adjustment with a 3-D translation stage to locate the peak field. The incident IR probe power was adjusted to maximize the signal. A transimpedance amplifier with a gain of 10^3 and bandwidth of 500 kHz converts the detector current to a voltage, which is terminated by 50 Ohms, and captured by a sampling oscilloscope. The peak value of this waveform is averaged for several pulses at each position in the delay scan.

In Fig. 4 (top), we show the EOS measurement of the near single-cycle THz pulse, followed in Fig. 4 (bottom) by the measurement using the PCA optimized for THz detection. The time delay between the initial, positive peak and second, negative peak was 0.33 ps for the EOS measurement and 0.53 ps for the PCA measurement. The PCA measurement provided a significantly better signal to noise ratio than the EOS technique. Using the standard deviation of the background signal, measured when the THz pulse was not temporally overlapped with the IR probe, we found a peak signal to noise ratio of 7.4×10^3 for the EOS measurement and 31.4×10^3 for the PCA measurement.

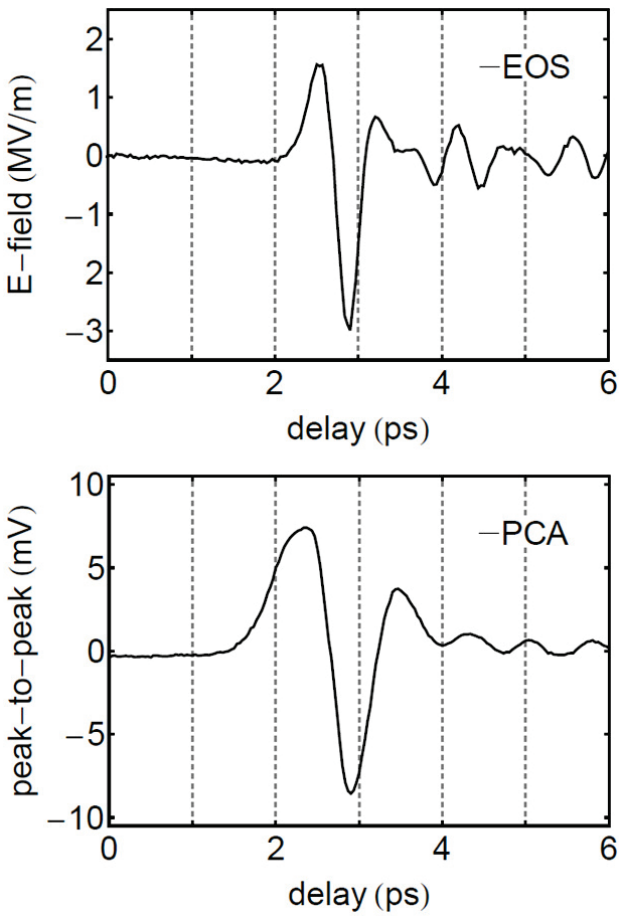

Figure 4: Measurements of the THz pulse using (top) EOS in a ZnTe crystal and (bottom) a PCA optimized for THz detection.

Accurately measuring the small signal currents generated by these devices has proven to be challenging in the accelerator noise environment, hence we seek to find detectors which produce the largest current outputs for a given THz and laser probe intensity. Two other plasmonic-enhanced devices were available and evaluated for accelerator/laser synchronizing applications. Despite the fact that these devices have a design optimized for THz emission, we compare the effect of increasing the active area by measuring the signal from a small and a large area devise.

The active area of the smaller photoconductive device is 0.5 mm × 0.5 mm. The second device is a larger version, 4 times in size, with an active area of 1 mm × 1 mm. These two devices were designed to operate with high-bias voltage, a property required for use as a high-power THz emitter, as described in [8]. The delay scan is shown in Fig. 5. The large peak signal provided by the 1 mm^2 PCA, in this case nearly a factor of two greater than the smaller area device, may be key to overcoming the noise background during a beam test. However, the signal to noise ratio *decreased* by 30 %, from 3.5×10^3 for the small area device to 2.5×10^3 in the case of the larger active area. In each case, this signal to noise ratio is roughly a factor of 10 worse than we measured using the chip optimized for detection.

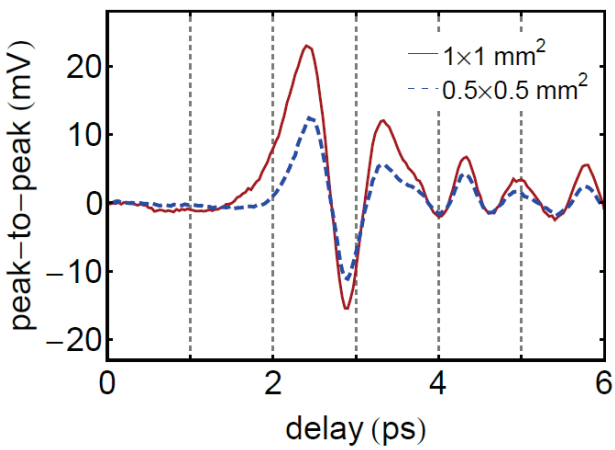

Figure 5: Measurements of the THz pulse using two PCA's, optimized for THz emission, with large (solid red) and small (dashed blue) area.

To summarize these measurements, we have found that each devise examined reproduces the near-single cycle THz waveform with features in close agreement with the reconstruction from the EOS method. The devise optimized for detection exhibits the highest signal to noise ratio. Using two devices optimized for THz emission, we find that the sensitivity increases with the active area, but at the cost of lower signal to noise over the first device.

ROBUST NOISE REDUCTION

Electronic background noise in the accelerator lab environment presents significant challenges for measuring the small current output of photoconductive detector. Ambient RF from the accelerator drive system and transient ground currents induced by the high voltage pulses delivered to the klystron are the two main noise sources com-

ISBN 978-3-95450-177-9

peting with the detector output. Therefore, steps have been taken to isolate the signal.

The detector chip is mounted on a two-layered printed circuit board (PCB) with epoxy and electrically connected by wire bonds to signal trace covered by solder mask. Bare gold cladding covering the top and bottom layers of the PCB provide ground isolation around the chip and traces, as well as preventing the accumulation of charge from any scraped beam halo.

Shielding within and outside of the beam vacuum chamber is achieved using triaxial cables. The two inner conductors carry the detector current while the outermost conductor is tied to ground. Signal leaves the PCB through a 50-Ohm triaxial connector (Fig. 6). An in-vacuum triaxial cable connects the PCB to a triaxial feedthrough. An air-side triaxial cable transports the signal to the amplifier.

Figure 6: CAD rendering of the THz detector PCB mounted on a retractable mechanical feedthrough to bring the chip near the electron beam (blue arrow). The probe laser (red arrow) enters the vacuum chamber through a viewport (not shown). With the tee suppressed (right), the triaxial signal coupling can be seen.

The THz detector is mounted on a movable actuator for positioning the sensor directly below the beam. The longitudinal component of the relativistic electron beam's Coulomb field is transformed into the radial component forming the so-called "pancake" distribution, producing a time-varying electric field radially polarized with THz bandwidth in the lab frame. The antenna array in the sensor couples to linearly polarized THz. Therefore, to sample the correct polarization over the active area, the sensor is to be positioned just below the beam with the thin edge aligned to the beam vector. In this case, the THz is vertically polarized at the chip. The system will mount to a cross on the PEGASUS beamline at UCLA with a viewport for coupling the laser into the vacuum chamber, where it strikes the large-area detector.

The laser probe must be linearly polarized with its field oscillating in the horizontal direction, 90 degrees with respect to the THz field. The spatial alignment of the beam spot on the detector is not critical, as opposed to PCA devices with conventional antennas where a ~10 μm spot must be placed within a ~10 μm gap in the single antenna structure. The large area of the device greatly reduces the complications in alignment of using the plasmonics-enhanced THz detector for in-vacuum applications.

CONCLUSION

We have considered beam and laser synchronization using plasmonics-enhanced large-area photoconductive detectors. Our experiences have shown that the transient RF and high-voltage noise background present in accelerator enclosure environments requires both highly shielded cables and feedthroughs for signal isolation as well as higher sensitivity PCA devices. Three newly fabricated designs have been PCB mounted and characterized using a bench-top pulsed THz source. The combination of enhanced sensitivity and noise reduction will be evaluated in upcoming beam test to measure the Coulomb THz field from the PEGASUS beam at UCLA this year.

REFERENCES

[1] A. Angelovski *et al.*, "Evaluation of the cone-shaped pickup performance for low charge sub-10 fs arrival-time measurements at free electron laser facilities," *Phys. Rev. ST Accel. Beams,* vol 18, p. 012801, Jan. 2015.

[2] M. Brunken *et al.,* "Electro-optic sampling at the TESLA test accelerator: experimental setup and first results," TESLA Report 2003-11, 2003.

[3] K. Kan *et al.*, "Measurement of temporal electric field of electron bunch using photoconductive antenna", in *Proc. IPAC'16*, Richmond, VA, USA, May 2015, pp. 1623-1625.

[4] K. Kan *et al.*, "Radially polarized terahertz waves from a photoconductive antenna with microstructures," *Appl. Phys. Lett.,* vol 102, p. 221118, June 2013.

[5] E.J. Curry, B.T. Jacobson, A.Y. Murokh, and P. Musumeci, "Sub-picosecond shot-to-shot electron beam and laser timing using a photoconductive THz antenna", in *Proc. IBIC'15*, Melbourne, Australia, September 2015, pp. 243-245.

[6] D. Cesar *et al.,* "Demonstration of single-shot picosecond time-resolved MeV electron imaging using a compact permanent magnet quadrupole based lens," *Phys. Rev. Lett.,* vol 117, p. 024801, July 2016.

[7] W. Berry, N. Wang, M. R. Hashemi, M. Unlu, and M. Jarrahi, "Significant performance enhancement in photoconductive terahertz optoelectronics by incorporating plasmonic contact electrodes," *Nat. Comm.,* vol 4, 1622, Mar 2013.

[8] N. T. Yardimci, S. H. Yang, C. W. Berry, and M. Jarrahi, "High-power terahertz generation using large-area plasmonic photoconductive emitters," *IEEE Trans. THz Sci. Technol*., vol 5, pp. 223-229, Mar 2015.

ISBN 978-3-95450-177-9